Nano Energy 23 (2016) 27–33

Contents lists available at ScienceDirect

Nano Energy

journal homepage: www.elsevier.com/locate/nanoenergy

Enhanced performances of flexible ZnO/perovskite solar cells by piezo-phototronic effect

Guofeng Hu [a,1], Wenxi Guo [a,1], Ruomeng Yu [b], Xiaonian Yang [a], Ranran Zhou [a], Caofeng Pan [a,*], Zhong Lin Wang [a,b]

[a] Beijing Institute of Nanoenergy and Nanosystems, Chinese Academy of Sciences, Beijing 100083, China
[b] School of Materials Science and Engineering, Georgia Institute of Technology, Atlanta, GA 30332-0245, USA

ARTICLE INFO

Article history:
Received 9 November 2015
Received in revised form
3 February 2016
Accepted 28 February 2016
Available online 2 March 2016

Keywords:
Perovskite solar cells
ZnO microwire
Piezo-phototronic effect

ABSTRACT

In this work, piezoelectric ZnO microwire was utilized to form heterojunctions with perovskite as flexible photovoltaic devices, and has a power conversion efficiency of 0.0216%. By employing the piezo-phototronic effect, the strain-induced piezoelectric polarization charges at the vicinity of ZnO/perovskite interface can modulate the transport and separation processes of photo-generated carriers within the photovoltaic device and enhance the performances of ZnO/perovskite solar cells. The corresponding open-circuit voltage (V_{oc}), short-circuit current (I_{sc}) and efficiency of the solar cells were improved by 25.42%, 629.47% and 1280% (from 0.0216% to 0.298%) through piezo-phototronic effect, respectively. Physical working mechanism behind the observed results was carefully investigated by using energy band diagram. This study provides a promising approach to effectively enhance the overall performances of flexible solar cells for various applications.

1. Introduction

Compared with conventional fossil fuels, solar energy is a reliable and green energy and therefore become a promising solution to the threat of global energy crises. The recent emergence of efficient solar cells based on organic/inorganic lead halide perovskite have been recognized as one of the prospective next-generation photovoltaics due to their high absorption coefficients, excellent charge transport properties and long exciton diffusion lengths [1–5]. Motivated by the goal of fabricating stable, high-efficiency and cost-effective perovskite solar cells, tremendous efforts have been devoted to improve the performance. To date, different strategies have been adopted for performance improvement, including the compositional engineering of perovskite materials, interfacial engineering of active layers, and configuration engineering of cell devices [6–12]. Although over 19% power conversion efficiency (PCE) has been attained within several years since its birth, there is still plenty of room for further improvement in efficiency [2,13,14]. Among these efforts, piezo-phototronic effect is a new but effective one, which has been demonstrated very effective for improving the performance of piezoelectric semiconductor nanowires solar cells [18–22]. For piezoelectric semiconductor NWs, such as ZnO, CdS and GaN, which possesses semiconducting and piezoelectric properties simultaneously, a piezoelectric potential is created inside the NW by applying a strain/pressure/force owing to the non-central symmetric crystal structure. *Piezo-phototronic effect* is to use this inner-crystal piezopotential as a "gate" voltage to tune/control the charge generation, separation, transport and/or recombination in optoelectronic processes. This effect has been utilized to enhance the performance of a photocell [14–16], sensitivity of a photodetector [17–19], and the external efficiency of an LED [20,23].

In this work, ZnO/perovskite solar cells (ZPSC) were fabricated by employing single ZnO microwire (MW) as the electron transporter on a flexible substrate, and the piezo-phototronic effect was investigated on these ZPSCs by introducing externally strains to the devices. When the *c*-axis of the ZnO NW pointed towards perovskite, the corresponding open-circuit voltage (V_{oc}) and short-circuit current (I_{sc}) of the solar cells were improved by 25.42% and 629.47%, respectively; while the power conversion efficiency was enhanced by 1280% (from 0.0216% to 0.298%) under a compressive strain of 0.8%. A theoretical model is proposed to explain the enhancement of the performance of the PV devices by the piezo-phototronic effect using energy band diagrams, in which the ZnO/perovskite solar cells were treated as a p–n junction. The effect of the polarity of the ZnO MW on the piezo-phototronic effect was first time experimentally proved. This work offers a good method for improving solar energy conversation efficiency by designing the orientation of the nanowires and the strain to be purposely

* Corresponding author.
E-mail address: cfpan@binn.cas.cn (C. Pan).
[1] Authors contributed equally to this work.

http://dx.doi.org/10.1016/j.nanoen.2016.02.057
2211-2855/

introduced in the packaging of the solar cells, and also is significant for fully understanding the operational mechanisms of perovskite solar cells and provides a promising way to enhance the overall performance of a perovskite solar cell.

2. Experimental sections

The ZnO MWs used for ZPSCs were synthesized *via* a vapor-liquid-solid (VLS) process [23]. The structure and fabrication process of the ZPSCs are schematically illustrated in Fig. 1a and b, respectively. First, a long ZnO MW was attached on a flexible polystyrene (PS) substrate with one end of the MW fixed by silver paste, serving as the photoanode. Second, a layer of epoxy was coated on the photoanode to protect it from contaminations in the following processes. Third, a thin layer of perovskite film was coated on the other end of the ZnO MW, followed by heating at 70 °C for 15 min to obtain a good crystallinity $CH_3NH_3PbI_3$. Forth, a thin layer of 2,2′,7,7′-tetrakis (N,N-pdimethoxyphenylamino) -9,9′-spirobifluorene (spiro-MeOTAD) film and silver paste were consecutively deposited on the perovskite as a hole transport material (HTM) and a counter electrode, respectively. The precursor solution of $CH_3NH_3PbI_3$ and spiro-MeOTAD were prepared following the previously reported procedures [5,24]. Finally, a layer of epoxy was applied to pack the whole device for better stability and performances. An optical microscope and a digital image of the as-fabricated device are shown in Fig. 1c and d, respectively.

The experimental set-up was shown in Fig. 1e. One end of the device was fixed tightly on a sample holder, the piezo-phototronic effect was introduced by bending the other end of the device through moving a positioner, which was attached to a 3D mechanical stage (with a displacement resolution of 1 μm) to produce compressive/tensile strains. The external strains applied to the device can be calculated according to the work reported by Yang and Zhou [25,26]. Light illuminations were provided by an AM 1.5 solar simulator (300 W model 91260, Newport). Under simulated air mass (AM) 1.5 solar illuminations of 100 mW cm^{-2} light intensity, the performances of the device under different strains were measured by a computer-controlled measurement system. The light intensities ranging from 8.71 to100 mW cm^{-2} were obtained by using a set of filters during the experiment.

3. Results and discussion

The morphology of ZnO MWs is characterized by SEM as shown in Fig. 2a, with length and diameter of several hundred micrometers and hundreds of nanometers, respectively.

An over-focused image of the ZnO NW is presented in Fig. 2b, together with a dual beam selected area electron diffraction pattern of the ZnO MWs, which clearly indicates that the ZnO MWs have a growth direction along *c*-axis, that is (0001) or (000-1).

The polarity of the ZnO MWs has been investigated by electron energy loss spectroscopy (EELS) [27]. In our experiments, a zero loss spectrum and the corresponding core–shell ionization edge EELS spectrum was obtained consecutively from the same region and dealt with using EL/P 3.0 software. The ZnO NW was tilted to the Bragg position of either (0002) or (000-2), and away from any zone axis but satisfying two-beam condition. The EELS spectra (Fig. 2c) were acquired from the reflection pattern A (the red curve in Fig. 2c) and the reflection pattern B (the black curve in Fig. 2c), respectively. The EELS spectra are with background subtracted according to the power law, and the multiple-inelastic-scattering effect removed using the Fourier ratio (for deconvolution)

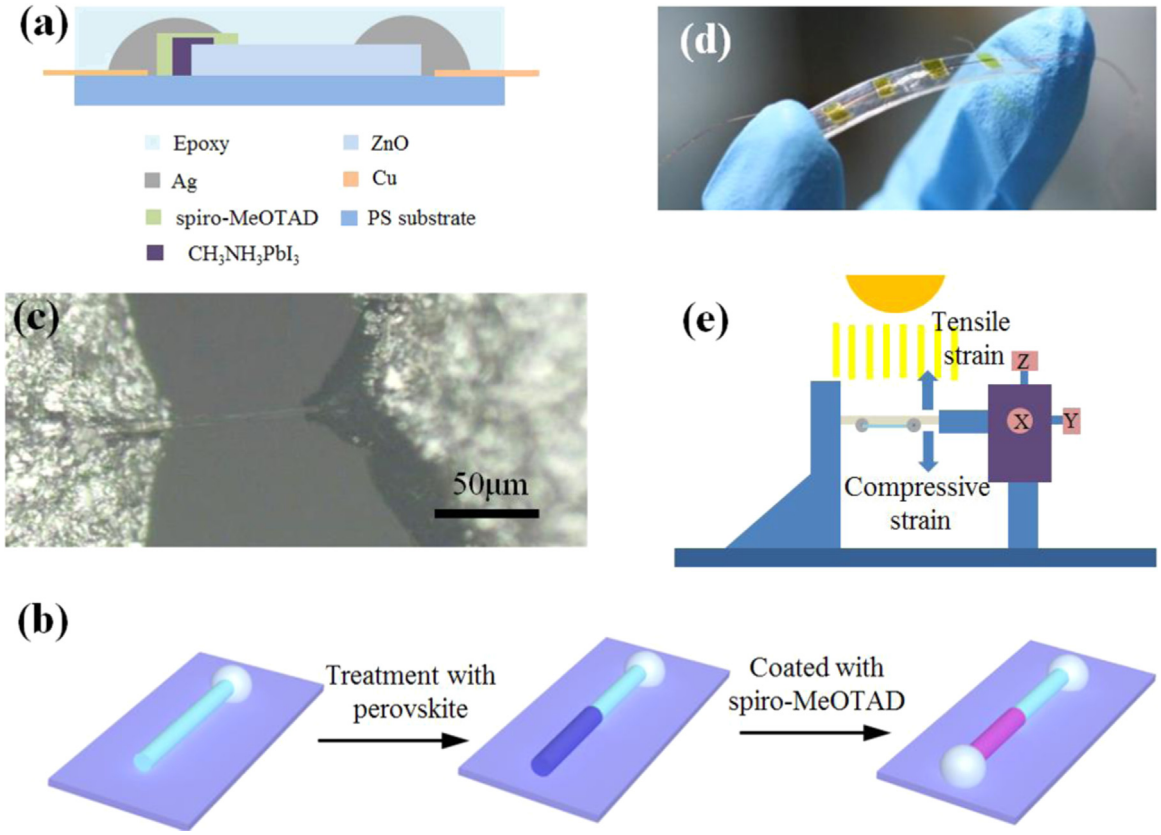

Fig. 1. (a) Schematic of a fabricated device. (b) Schematic of the fabrication process. (c, d) Optical microscopy and digital image of a typical device. (e) Schematic of the measurement set-up.

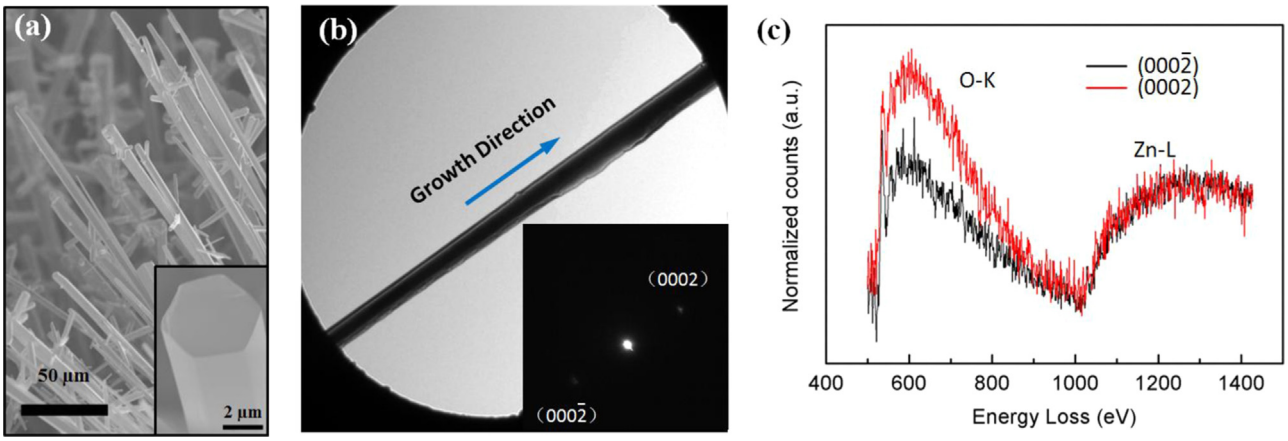

Fig. 2. (a) Scanning electron microscopy (SEM) image of the as-grown ZnO NWs; Inset: enlarged SEM image of an individual ZnO NW, showing a perfect hexagonal cross-section. (b) The shadow image of the ZnO MW in the over-focused SAED pattern of ZnO NW; Inset: corresponding electron diffraction pattern. (c) Comparison of the normalized O *K* -edges acquired at (0002) and Bragg conditions.

technique. The Zn $L_{2,3}$-edge spectra are normalized to compare the two O K-edge intensities. It is obvious that a stronger O K-edge intensity observed in red curve indicates the (0002) Bragg orientation. Then, According to the two-beam theory for acentric crystals which is employed to clarify the EELS result and determine the polarity of the ZnO film, the O-K edge taken at the (0002) Bragg condition should be higher than that at the (000-2) Bragg condition when the spectra are normalized using the Zn L-edges [27]. As a result, reflection pattern A can be indexed as (0002), while the reflection pattern B can be indexed as (000-2). Together with the shadow image of ZnO MW in the over-focused selected area electron diffraction (SAED) pattern, we can conclude that the growth direction of the ZnO MW is $+c$ axis.

Typical *I–V* Characteristics of ZPSCs were investigated under different light intensities as applying no strain (Fig. 3a) and a 0.47% tensile strain (Fig. 3b). It is obvious that the general performances of ZPSCs were significantly improved by applying an external strain under different light illumination conditions. The corresponding photovoltaic parameters, such as open-circuit voltage (V_{oc}), short-circuit current density (I_{sc}), and conversion efficiency (η) *versus* light intensities are analyzed and summarized in Fig. 3c and d. It can be observed that with increasing the light intensities,

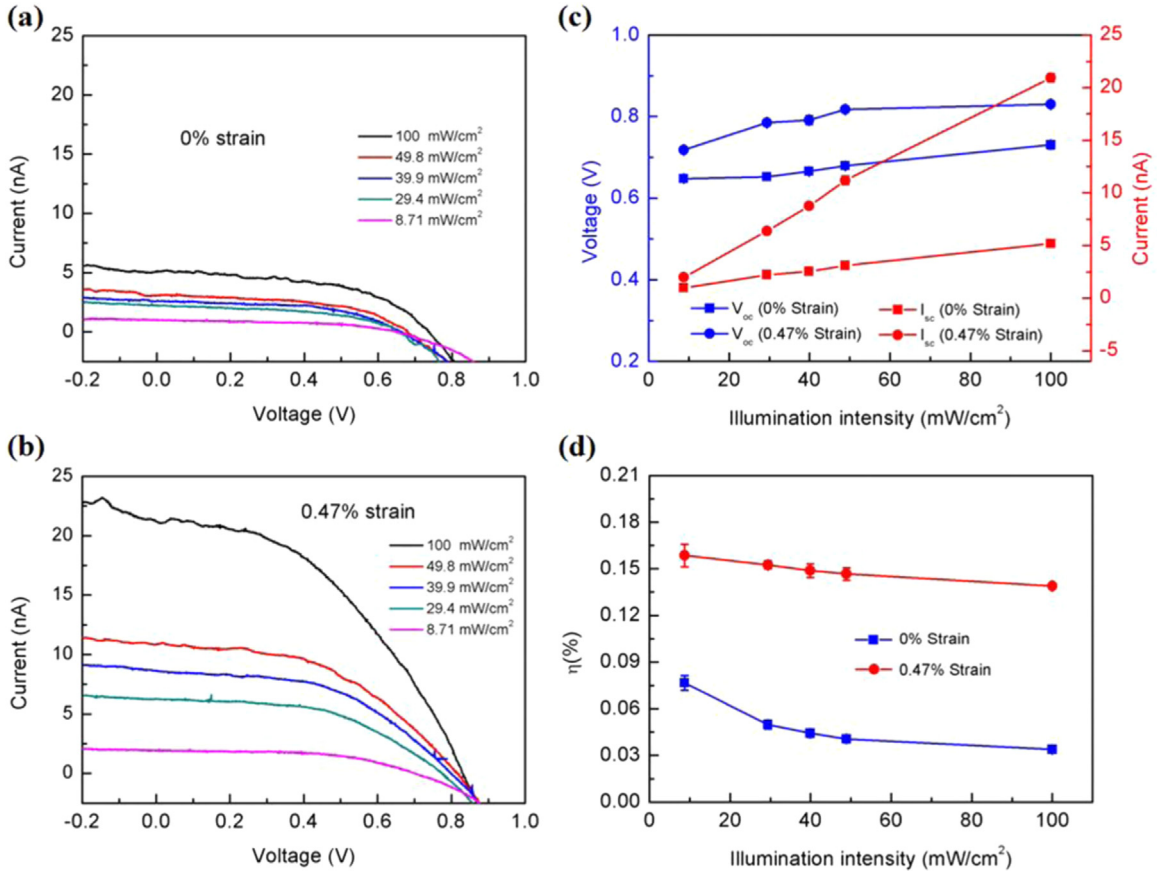

Fig. 3. (a, b) *I–V* curves of the device under different illuminations in the condition of 0% strain (a), 0.47% strain (b). (c, d) Dependence of the open circuit voltage and the short circuit current (c), efficiency (d) under compressive strain in condition of different strains.

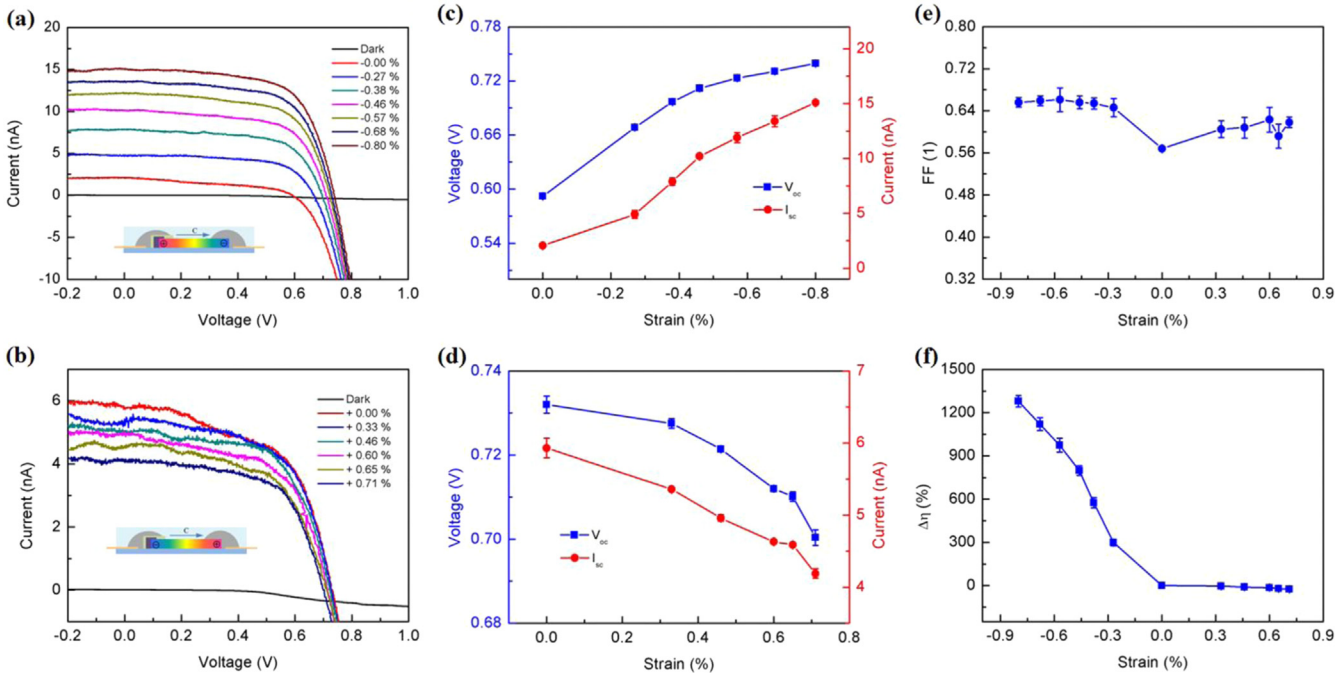

Fig. 4. The performance for the ZPSC-I device. (a, b) *I–V* curves of the device under compressive strain (a), and under stretch strain (b). (c, d) Dependence of the open circuit voltage and the short circuit current under compressive strain (c), and under stretch strain (d). (e, f) Dependence of the fill factor (e), and relative efficiency change (f) on the strains.

the V_{oc} increased from 0.65 to 0.73 V under strain-free condition (Fig. 3c), while increased from 0.71 to 0.83 V under 0.47% tensile strain (Fig. 3c). Similarly, the I_{sc} increased from 0.97 to 5.20 nA without applying tensile strain, while increased from 2.00 to 20.94 nA under a 0.47% tensile strain. Moreover, the power conversion efficiency η, which is defined as $\eta = FF^{*}V_{oc}{}^{*}I_{sc}/(P_{in}{}^{*}A)$, where P_{in} is the incident light density, A is the effective illumination area (Fig. S1), FF is the fill factor, is higher under each light intensity after applying 0.47% tensile strain, as shown in Fig. 3d. It can be found that η increased from 0.0338% to 0.139% (0.47% strain) under a full-sun intensity (100 mW cm^{-2}). These results clearly indicate the enhancements on performances of ZPSCs by piezo-phototronic effect.

To systematically investigate the piezo-phototronic effect enhancements on the performances of ZPSCs, continuous and variable external strains were applied on the devices and the corresponding results are presented in Fig. 4 and 5. The measured ZPSCs devices were divided into two categories based on the *c*-axis direction of the ZnO MWs with respect to perovskite [15,28]: devices with the *c*-axis of ZnO pointing away from perovskite are marked

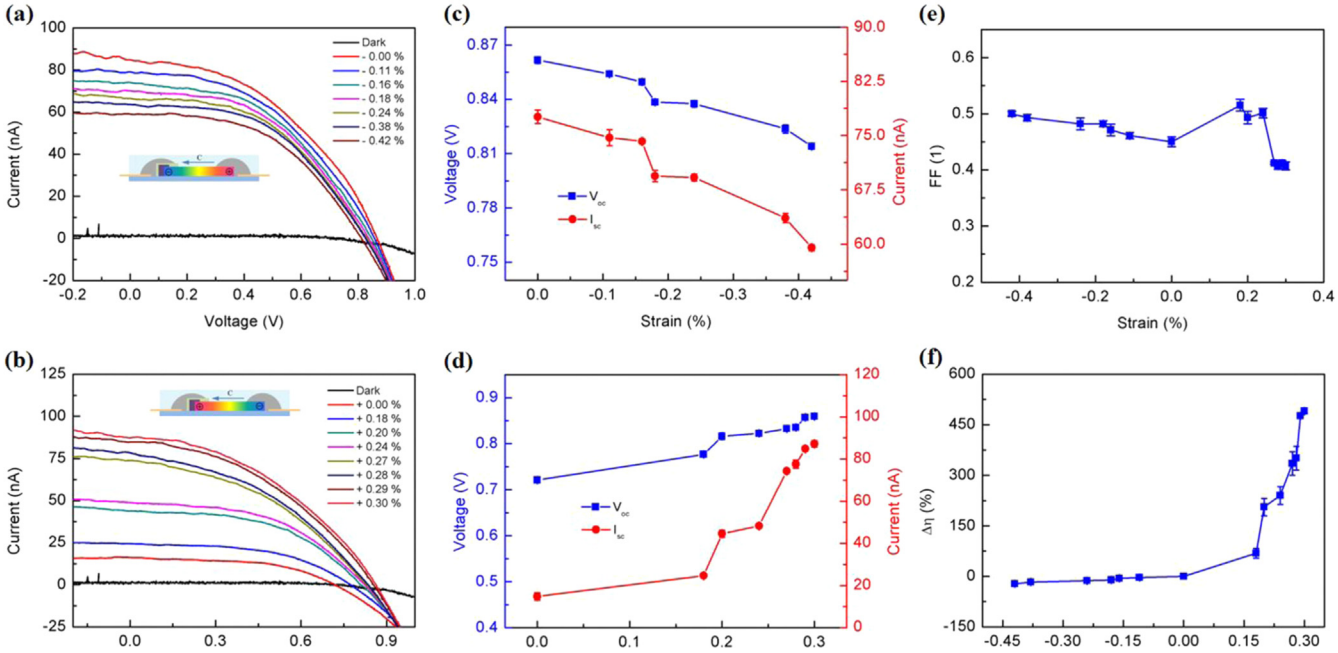

Fig. 5. The performance for the ZPSC-II device. (a, b) *I–V* curves of the device under compressive strain (a), and under stretch strain (b). (c, d) Dependence of the open circuit voltage and the short circuit current under compressive strain (c), and under stretch strain (d). (e, f) Dependence of the fill factor (e), and relative efficiency change (f) on the strains.

as ZPSC-I; devices with the *c*-axis of ZnO pointing towards perovskite are ZPSC-II. The piezo-phototronic effect on the performances of ZPSC-I device is illustrated in Fig. 4. The *I–V* curves of the ZPSCs subjected to compressive and tensile strains are presented in Fig. 4a and b, respectively. It is obvious that both the V_{oc} and I_{sc} increased as increasing compressive strains, and decreased as increasing tensile strains. The values of V_{oc} and I_{sc} under different strains were extracted and plotted in Fig. 4c and d, respectively. As shown in Fig. 4c, the V_{oc} increased from 0.59 to 0.74 V and the I_{sc} increased from 2.07 to 15.10 nA as increasing compressive strain from 0% to −0.8%. On the contrary, the V_{oc} decreased from 0.73 to 0.70 V and the I_{sc} decreased from 5.93 to 4.19 nA as increasing tensile strains from 0% to 0.71% (Fig. 4d). Opposite performances of ZPSCs were obtained from opposite strain conditions. Similar fill factors (FF) were derived under both compressive and tensile strains as shown in Fig. 4e. The power conversion efficiency increased from 0.0216% to 0.298% as increasing the compressive strain from 0% to −0.8%, corresponding to a relative enhancement of 1280% in efficiency by piezo-phototronic effect.

The piezo-phototronic effect on the performances of ZPSC-II is presented in Fig. 5. Different from ZPSC-I, opposite optoelectronic behavior were observed for ZPSC-II devices, since the direction of *c*-axis was reversed. Both the V_{oc} and I_{sc} decreased as increasing compressive strains, and increased as increasing tensile strain, as shown in Fig. 5a and b. The V_{oc} decrease from 0.86 to 0.81 V, and the I_{sc} decreased from 77.60 to 59.50 nA under a −0.42% compressive strain, as shown in Fig. 5c. As shown in Fig. 5d, the V_{oc} increased from 0.72 to 0.86 V, and I_{sc} increased from 14.80 to 87.20 nA under a 0.30% tensile strain. The fill factors of ZPSC-II increased as increasing compressive strains, while presented no obvious trend under tensile strains as shown in Fig. 5e. The power conversion efficiency increased from 0.068% to 0.352% as a tensile strain increasing from 0% to 0.30%, corresponding to a relative enhancement of 417.650% in efficiency as shown in Fig. 5f. The opposite modifications on ZPSCs' performances by external strains observed from both types of devices confirm the dominance of piezo-phototronic effect, instead of piezo-resistive effect, which is a nonpolar volume effect.

According to the Shockley equivalent circuit [15,18], the *I–V*

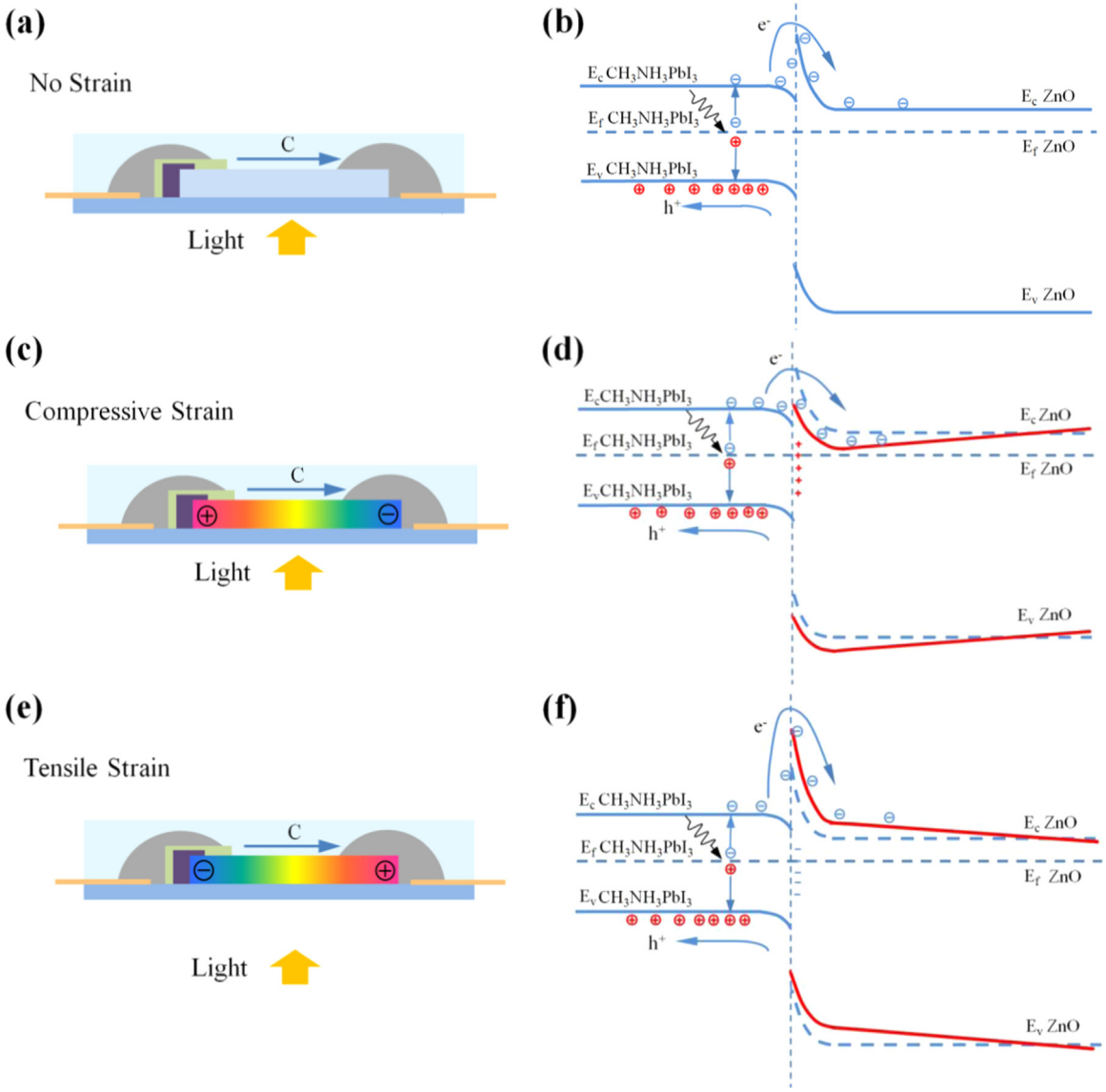

Fig. 6. Schematics and energy band diagrams demonstrate the piezo-phototronic effect on perovskite/ZnO single micro/nanowire solar cells. (a) The piezo-potential distributions for a strain-free device, and (b) the corresponding energy band diagram. (c) The piezo-potential distributions in the compressed device of [0001] (ZPSC-I) and in stretched device of [000-1] (ZPSC-II), and (d) the corresponding energy band diagram. (e) The piezo-potential distributions in the stretched device of [0001] (ZPSC-I) and in compressed device of [000-1] (ZPSC-II), and (f) the corresponding energy band diagram.

characteristic of ZPSC are described as

$$I_{sc} = qG(L_n + L_p) \tag{1}$$

$$V_{oc} = \frac{kT}{q} \ln\left(\frac{I_{sc}}{I_{pn0}\exp\left(\frac{-\Delta E}{rkT}\right)}\right) \tag{2}$$

In Eq. (1), the G is the electron–hole pair generation rates, L_n and L_p are the electron and hole diffusion lengths respectively. It indicates that reduction of the possibility of recombination caused by piezo-phototronic effect may result in an increase of I_{sc} under a fixed value of G. In Eq. (2), I_{pn0} is a prefactor, r is the ideality factor, and ΔE is the energy band difference between the conduction band of a n-type inorganic material and the conduction band of a p-type organic material. In our experiment, the change of ΔE at the vicinity of ZnO/perovskite interface under different strains may lead to the variety of V_{oc}. And, the variety of V_{oc} depends on the changes of ΔE and I_{sc}. The varieties of I_{sc} and V_{oc} are in agreement with the result expected by piezo-phototronic effect.

To better understand the physical mechanism behind the observed optoelectronic performances at the ZnO/perovskite interface, a theoretical model was proposed to explain the piezo-phototronic effect on the performance of ZPSCs using energy band diagrams, as shown in Fig. 6. Under strain-free condition, a heterojunction is formed between ZnO and perovskite, as shown in Fig. 6a and b, a strain-free device is presented in Fig. 6a and b. The performance of ZPSC-I and ZPSC-II were equivalent in a ZPSC under a strain-free condition [29]. For a typical device, the main physical processes governing the cell behavior are shown in Fig. 6b. The perovskite $CH_3NH_3PbI_3$ has a direct bandgap about 1.5 eV, corresponding to an absorption onset of 800 nm [30]. In this regard, the electron–hole pairs are mostly generated in the $CH_3NH_3PbI_3$ under illumination and then the generated electron–hole pairs are separated under the built-in electric field across the depletion region with electrons transferring to the ZnO MW, and the holes transferring to the HTM layer.

When the ZnO MW is subjected to strain, the energy band at the ZnO interface will change by piezoelectric effect. It was proved by numerous studies about ZnO, GaN nanogenerators and piezotronics [31,32]. As shown in Fig. 6c, a strain-induced positive piezoelectric charge will occur at the perovskite/ZnO interface when ZPSC-I is subjected to compressive strain or ZPSC-II is subjected to tensile strain. As shown in Fig. 6d, the local piezoelectric charges will lower both of the conduction and valence bands of ZnO at the interface, leading to a decrease of the barrier height at the perovskite/ZnO interface. It increases the depletion width and strengthens the built-in electric field, increasing separation efficiency of the electron–hole pair and decreasing the possibility of recombination. Thus, the performance of the solar cell is enhanced.

On the contrary, a strain-induced negative piezoelectric charge will occur at the perovskite/ZnO interface when ZPSC-I is subjected to tensile strain or ZPSC-II is subjected to compressive strain, as shown in Fig. 6e. In Fig. 6f, the local piezoelectric charges will lift up both the conduction and valence bands of ZnO at the interface, leading in an increase of the barrier height at the perovskite/ZnO interface. It reduces the depletion width and weakens the strength of built-in electric field, decreasing separation efficiency of the electron–hole pair and increasing the possibility of recombination. Thus, the convention efficiency is decreased. This is the basic mechanism to interpret how does the piezo-phototronic effect tunes the performance of a solar cell.

The stability of these ZPSCs were investigated by monitoring the performances of the device operated under 0% strains and AM 1.5 illuminations for over 1 h, as shown in Fig. S2. The output current was stable at 13.5 nA throughout the whole measurement with less than 10% deviation, indicating a reliable stability of our ZPSCs. This stability tests revealed clearly that the devices were stable enough to carry out investigation on strain-solar cell performance, which cost about half an hour. It indicated that the enhancement of the performance was induced by the piezo-phototronic effect, and was not for instability or other electronic condition disturbing [33].

4. Conclusions

In summary, a flexible ZPSC was designed and fabricated by employing single ZnO microwire as the electron transporter. By externally applying strains on the devices, piezo-phototronic effect has been introduced to enhance the general performances of ZPSCs. The corresponding open-circuit voltage (V_{oc}) and short-circuit current (I_{sc}) of the solar cells were improved by 25.42% and 629.47%, respectively. The power conversion efficiency was enhanced from 0.0216% to 0.298% (by 1280%) through piezo-phototronic effect. A theoretical model was carefully studied to explain the performance of the solar cells using the energy band diagram. This work is important for fully understanding the operational mechanisms of perovskite solar cells and provides a promising way to enhance the overall performance of a flexible solar cell.

Appendix A. Supplementary material

Supplementary data associated with this article can be found in the online version at http://dx.doi.org/10.1016/j.nanoen.2016.02.057.

References

[1] N.G. Park, J Phys. Chem. Lett. 4 (2013) 2423–2429.
[2] H.J. Snaith, J Phys. Chem. Lett. 4 (2013) 3623–3630.
[3] A. Kojima, K. Teshima, Y. Shirai, T. Miyasaka, J. Am. Chem. Soc. 131 (2009) 6050–6051.
[4] J. Burschka, N. Pellet, S.J. Moon, R. Humphry-Baker, P. Gao, M.K. Nazeeruddin, M. Grätzel, Nature 499 (2013) 316–319.
[5] D.Y. Liu, T.L. Kelly, Nature Photon. 8 (2014) 133–138.
[6] N.J. Jeon, J.H. Noh, W.S. Yang, Y.C. Kim, S. Ryu, J. Seo, S.I1 Seok, Nature 517 (2015) 476–480.
[7] M.Z. Liu, M.B. Johnston, H.J. Snaith, Nature 501 (2013) 395–398.
[8] W. Zhang, M. Saliba, D.T. Moore, S.K. Pathak, M.T. Hőrantner, T. Stergiopoulos, S.D. Stranks, G.E. Eperon, J.A. Alexander-Webber, A. Abate, A. Sadhanala, S. H. Yao, Y.L. Chen, R.H. Friend, L.A. Estroff, U. Wiesner, H.J. Snaith, Nat. Commun. 6 (2015) 6142.
[9] N.J. Jeon, J.H. Noh, Y.C. Kim, W.S. Yang, S. Ryu, S. Il Seol, Nature Mater. 13 (2014) 897–903.
[10] L. Etgar, P. Gao, Z.S. Xue, Q. Peng, A.K. Chandiran, B. Liu, Md.K. Nazeeruddin, M. Grätzel, J. Am. Chem. Soc. 134 (2012) 17396–17399.
[11] W. Zhang, M. Anaya, G. Lozano, M.E. Calvo, M.B. Johnston, H. Míguez, H. J. Snaith, Nano Lett. 15 (2015) 1698–1702.
[12] A.Y. Mei, X. Li, L.F. Liu, Z.L. Ku, T.F. Liu, Y.G. Rong, M. Xu, M. Hu, J.Z. Chen, Y. Yang, M. Grätzel, H.W. Han, Science 345 (2014) 295–298.
[13] H.P. Zhou, Q. Chen, G. Li, S. Luo, T.B. Song, H.S. Duan, Z.R. Hong, J.B. You, Y.S. Liu, Y. Yang, Science 345 (2014) 542–546.
[14] R.F. Service, Science 342 (2013) 794–797.
[15] Y. Zhang, Y. Liu, Z.L. Wang, Adv. Mater. 23 (2011) 3004–3013.
[16] W.Z. Wu, L. Wang, Y.L. Li, F. Zhang, L. Lin, S.M. Niu, D. Chenet, X. Zhang, Y. F. Hao, T.F. Heinz, J. Hone, Z.L. Wang, Nature 514 (2014) 470–474.
[17] Z.L. Wang, Nano Today 5 (2010) 540–552.
[18] Y. Yang, W.X. Guo, Y. Zhang, Y. Ding, X. Wang, Z.L. Wang, Nano Lett. 11 (2011) 4812–4817.
[19] C.F. Pan, S.M. Niu, Y. Ding, L. Dong, R.M. Yu, Y. Liu, G. Zhu, Z.L. Wang, Nano Lett. 12 (2012) 3302–3307.
[20] X.N. Wen, W.Z. Wu, Z.L. Wang, Nano Energy 2 (2013) 1093–1100.
[21] S. Shoaee, J. Briscoe, J.R. Durrant, S. Dunn, Adv. Mater. 26 (2014) 263–268.
[22] F. Boxberg, N. Sndergaard, H.G. Xu, Nano Lett. 10 (2010) 1108–1112.
[23] G. Zhu, Y.S. Zhou, S.H. Wang, R.S. Yang, Y. Ding, X. Wang, Y. Bando, Z.L. Wang, Nanotechnology 23 (2012) 055604.
[24] A. Marchioro, J. Teuscher, D. Friedrich, M. Kunst, R. van de Krol, T. Moehl, M. Grätzel, J.E. Moser, Nature Photon. 8 (2014) 250–255.

[25] R.S. Yang, Y. Qin, L.M. Dai, Z.L. Wang, Nature Nanotech. 4 (2009) 34–39.
[26] J. Zhou, P. Fei, Y.D. Gu, W.J. Mai, Y.F. Gao, R.S. Yang, G. Bao, Z.L. Wang, Nano Lett. 8 (2008) 3973–3977.
[27] Y. Wang, Q.Y. Xu, X.L. Du, Z.X. Mei, Z.Q. Zeng, Q.K. Xue, Z. Zhang, Phys. Lett. A 320 (2004) 322–326.
[28] Z.L. Wang, Adv. Mater. 19 (2007) 889–892.
[29] J. Shi, J. Dong, S. Lv, Y. Xu, L. Zhu, J. Xiao, X. Xu, H. Wu, D. Li, Y. Luo, Q. Meng, Appl. Phys. Lett. 104 (2014) 063901.
[30] T. Baikie, Y. Fang, J.M. Kadro, M. Schreyer, F. Wei, S.G. Mhaisalkar, M. Graetzel, T.J. White, J Mater. Chem. A 1 (2013) 5628–5641.
[31] Z.L. Wang, J.H. Song, Science 312 (2006) 242–246.
[32] W.Z. Wu, C.F. Pan, Y. Zhang, X.N. Wen, Z.L. Wang, Nano Today 8 (2013) 619–642.
[33] B.C. O'Regan, P.R. Barnes, X. Li, C. Law, E. Palomares, J.M. Marin-Beloqui, J. Am. Chem. Soc. 137 (2015) 5087–5099.

Guofeng Hu received the B.S. degree in School of Science from Tianjin Polytechnic University, China, in 2010. He is currently pursuing the Ph.D. degree at the Laboratory of piezo-phototronics, Beijing Institute of Nanoenergy and Nanosystems, Chinese Academy of Sciences. His research work is focusing on the fields of piezotronics/piezo-phototronics for fabricating new electronic and optoelectronic devices.

Dr. Wenxi Guo received his B.S. and Ph.D. degree in College of Chemistry and Chemical Engineering at Xiamen University in 2008 and 2014, respectively. Then, he had been an assistant research fellow in the group of Professor Caofeng Pan at Beijing Institute of Nanoenergy and Nanosystems, Chinese Academy of Sciences. He then joined School of Physics and Technology, Xiamen University and became an associate professor since 2015, His research focuses on the fields of flexible thin film solar cells and piezotronic/piezo-phototronic effects of nano-devices.

Ruomeng Yu is a Ph.D. candidate in School of Materials Science and Engineering at Georgia Institute of Technology, under the supervision of Prof. Zhong Lin Wang as a graduate research assistant. He received his B.S. degree in Applied Physics from Huazhong University of Science and Technology in 2010, and his M.S. degree in Physics from Georgia Institute of Technology in 2012. His research interests include synthesis, fabrication and integration of nanomaterials/electronic devices; nano/micro-scale electronics for energy harvesting/conversion/storage; self-powered sensing systems; mechanical/optical signals-controlled logic circuits; optoelectronics; piezotronics/piezo-photonics/piezo-phototronics.

Xiaonian Yang is a master student since 2014 under the guidance of Prof.Caofeng Pan in Beijing Institute of Nanoenergy and Nanosystems (BINN), Chinese Academy of Sciences, (CAS) China.She received her B. S. degree in School of Materials Science and Engeneering, Huazhong University of Science and Technology in 2014. Her current research interest concentrates on two-dimensional materials growth, corresponding device fabrication and their applications in nanoelectronics.

Ranran Zhou is a master student from 2013 under the guidance of Prof. Caofeng Pan in Beijing Institute of Nanoenergy and Nanosystems (BINN), Chinese Academy of Science, China. She received her B.S. degree in Materials science and engeneering from Zhengzhou University in 2013. Her current research interest is physical and chemical processes in nanomaterials growth, properties, fabrication of novel devices, and their unique applications in sensing systems and energy science.

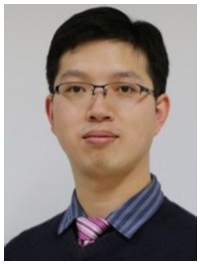

Dr. Caofeng Pan received his B.S. degree (2005) and his Ph.D. (2010) in Materials Science and Engineering from Tsinghua University, China. He then joined in the group of Professor Zhong Lin Wang at the Georgia Institute of Technology as a postdoctral fellow. He is currently a professor and a group leader at Beijing Institute of Nanoenergy and Nanosystems, Chinese Academy of Sciences since 2013. His main research interests focus on the fields of piezotronics/piezo-phototronics for fabricating new electronic and optoelectronic devices, nano-power source (such as nanofuel cell, nano biofuel cell and nanogenerator), hybrid nanogenerators, and self-powered nanosystems. He has published over 50 peer reviewed papers, with citation over 1000 and H-index of 19. Details can be found at http://piezotronics.binncas.cn/.

Dr. Zhong Lin (ZL) Wang is the Hightower Chair in Materials Science and Engineering, Regents' Professor, at Georgia Tech. He is also the chief scientist and director of Beijing Institute of Nanoenergy and Nanosystems, Chinese Academy of Sciences. Dr. Wang has made original and innovative contributions to the synthesis, discovery, characterization and understanding of fundamental physical properties of oxide nanobelts and nanowires, as well as applications of nanowires in energy sciences, electronics, optoelectronics and biological science. He is the leader figure in ZnO nanostructure research. His discovery and breakthroughs in developing nanogenerators establish the principle and technological road map for harvesting mechanical energy from environment and biological systems for powering a personal electronics. His research on self-powered nanosystems has inspired the worldwide effort in academia and industry for studying energy for micro-nano-systems, which is now a distinct disciplinary in energy research and future sensor networks. He coined and pioneered the field of piezotronics and piezo-phototronics by introducing piezoelectric potential gated charge transport process in fabricating new electronic and optoelectronic devices. This historical breakthrough by redesign CMOS transistor has important applications in smart MEMS/NEMS, nanorobotics, human-electronics interface and sensors. Wang also invented and pioneered the in-situ technique for measuring the mechanical and electrical properties of a single nanotube/nanowire inside a transmission electron microscope (TEM).